PHYSICAL REVIEW A **75**, 011604(R) (2007)

Arresting soliton collapse in two-dimensional nonlinear Schrödinger systems via spatiotemporal modulation of the external potential

Kestutis Staliunas,[1] Ramon Herrero,[2] and Germán J. de Valcárcel[3]
[1]*Institució Catalana de Recerca i Estudis Avançats (ICREA), Departament de Fisica i Enginyeria Nuclear, Universitat Politècnica de Catalunya, Colom 11, E-08222 Terrassa, Spain*
[2]*Departament de Fisica i Enginyeria Nuclear, Universitat Politècnica de Catalunya, Comte d'Urgell 187, E-08036 Barcelona, Spain*
[3]*Departament d'Òptica, Universitat de València, Dr. Moliner 50, E-46100 Burjassot, Spain*
(Received 18 March 2006; published 16 January 2007)

We predict stable, collapse-free solitonslike structures in two-dimensional nonlinear Schrödinger systems in subdiffractive regimes, accomplished by a spatiotemporal modulation of the external potential. We investigate the scaling laws, the stability, and the dynamical properties of these subdiffractive solitons.

DOI: 10.1103/PhysRevA.75.011604 PACS number(s): 03.75.Kk, 05.45.Yv

Nonlinear waves in two-(2D) and three-dimensional (3D) systems with self-focusing, or attracting, cubic interactions are subject to collapse [1]. Quoting Bergé [1] "wave collapse concerns the formation of singularities in the solutions of evolution equations governing the fate of nonlinear wave forms" in a finite blowup time. Obviously such discontinuity is not physical (other nonlinear interaction processes enter into play before the collapse, resulting in quintic, or higher order, models [2]) but anyway has a dramatic, negative effect on soliton stability [1]. Accordingly, ways to arrest collapse have been explored, such as the use of spatially periodic lattice potentials [3], or the management of diffraction [4]. Other, intrinsic effects, such as the nonlinearity nonlocality, have also proven to be effective in the collapse arresting [5]. In this paper we present an alternative way to yield stable solitons in 2D systems with cubic nonlinearity that applies, in particular, to optical and matter waves. The proposal is triggered by recent work on spatiotemporal modulation of one-dimensional (1D) systems [6,7], where it is demonstrated that the diffraction properties of the system can be manipulated in such a way that a "subdiffractive" regime, characterized by an almost absence of diffraction, leads [7] to unique 1D solitonic families. As in a hypothetical, diffraction-free case collapse cannot occur (there is no spatial coupling), we guess that subdiffractivity can help in stabilizing solitons. The rest of this paper is devoted to demonstrate, analytically and numerically, this conjecture.

We consider the following dimensionless, nonlinear Schrödinger equation (NLSE) in two spatial dimensions:

$$\partial_t \psi(\mathbf{r},t) = i[\nabla^2 + V(\mathbf{r},t) - |\psi|^2]\psi, \tag{1a}$$

$$V(\mathbf{r},t) = 4f\cos(\Omega_0 t)V_s(\mathbf{r}), \tag{1b}$$

$$V_s(\mathbf{r}) = \sum_{j=1}^{s} \cos(\mathbf{q}_j \cdot \mathbf{r}), \tag{1c}$$

where $\mathbf{r}=(x,y)$ denotes spatial coordinates, $\nabla^2 = \partial^2/\partial x^2 + \partial^2/\partial y^2$ is the Laplace operator, and t is the evolution parameter, which we call time. The external potential V is periodically (harmonically) modulated both in time, with frequency Ω_0, and in space, where it is given by the superposition of s lattices of wave vectors $\{\mathbf{q}_j\}_{j=1}^{s}$ of equal length ($|\mathbf{q}_j|=1$ without loss of generality) rotated each other by π/s, corresponding to potentials of $2s$-fold spatial symmetry. Finally f denotes the potential modulation amplitude.

The NLSE (1) applies to two basic physical problems: On the one hand it describes the dynamics of 2D BECs with repulsive atomic interactions in countermoving potential lattices represented by V [8], in which case t denotes true time. On the other hand (1) describes the paraxial propagation of monochromatic light beams through 3D defocusing PCs [here "time" t plays the role of the spatial propagation coordinate, usually denoted by z, and the spatial coordinates $\mathbf{r}=(x,y)$ are transverse to it] whose linear refractive index modulation is proportional to V [9].

In order to understand why stable 2D solitons of (1) are found we note that, in the limit of weak potential modulation and weak nonlinearity, and when the modulation parameters are properly tuned, solutions of (1) exist in the form $\psi(\mathbf{r},t) = A(\mathbf{r},t)\psi_B(\mathbf{r},t)$, $\psi_B(\mathbf{r},t)$ being a Bloch mode of the linear part of (1a) characterized by a null quasimomentum, and $A(\mathbf{r},t)$ a complex envelope of the Bloch mode. In the 1D case [7] the envelope equation is a modified NLSE of the form

$$\partial_t A(\mathbf{r},t) = i[d_2\partial_x^2 + d_4\partial_x^4 - |A|^2]A, \tag{2a}$$

which contains both a second-order spatial derivative (the usual diffraction operator) and a fourth-order one, signaling subdiffraction [6,7]. In 2D geometries one can expect a similar result, i.e.

$$\partial_t A(\mathbf{r},t) = i[d_2\nabla^2 + d_4\nabla^4 - |A|^2]A, \tag{2b}$$

which, remarkably, supports stable 2D solitons [10]. Here we give arguments to understand those results in [10], based on scaling arguments. In the purely subdiffractive case $d_2=0$ and $d_4=1$ (set to unity after normalization), and assuming a localized, bell-shaped solution with peak amplitude A_0, width r_0, and chemical potential (or propagation constant) μ, the following relations follow from (2b): $A_0^2 r_0^4 = \text{const}$ and $\mu r_0^4 = \text{const}$. Alternatively, in terms of the normalized number of particles (photons in case of optics, or condensed atoms in BECs), $N_0 = \int d^2 r |A|^2$, the above solitonic relations become $N_0 r_0^2 = \text{const}$ and $\mu N_0^{-2} = \text{const}$, where the constants, of order of one, depend on the precise definition of r_0. Finally, the

Vakhitov-Kolokolov criterion [10,11], which requires $dN_0/d|\mu|>0$ for the (generalized) NLSE solitons to be stable, clearly predicts the existence of stable solitons in the 2D subdiffractive NLSE.

However the 2D case is more involved than the 1D case and the transformation $\partial^2/\partial x^2 \to \nabla^2$ used in the passage from (2a) to (2b) above needs not be right. Hence our first goal is to determine under which conditions the envelope satisfies the subdiffractive NLSE (2b), what is tightly related with the properties of the Bloch modes of the linear part of (1a) [12]. These modes can be written as $\psi_B(\mathbf{r},t) = \exp[i(\mathbf{K}\cdot\mathbf{r}-\Omega t)]P(\mathbf{r},t)$ [6,7], being $\mathbf{K}=(K_x,K_y)$ the Bloch mode quasimomentum and Ω its quasienergy (quasipropagation constant in PCs or quasichemical potential in BECs), and P a function of space and time, formed by the superposition of periodic functions (in 1D such function is strictly periodic). A simple group-theory argument allows us to identify the kind of spatial potentials, Eq. (1c), that can lead to an envelope equation such as (2b), as follows. We remind everyone that we are assuming the $\mathbf{q}_j$'s to be rotating each other by π/s, corresponding to potentials of $2s$-fold symmetry. This implies that the quasienergy Ω of any Bloch mode must be invariant under π/s-rotations of the quasimomentum $\mathbf{K}$. For small $|\mathbf{K}|$, which is the case of interest [12], a Taylor expansion is justified

$$\Omega = \alpha_x K_x^2 + \alpha_y K_y^2 + \alpha_{xx} K_x^4 + \alpha_{xy} K_x^2 K_y^2 + \alpha_{yy} K_y^4 + \cdots, \quad (3)$$

where only even powers of the quasimomentum are considered owed to the reflection symmetry of (1). Imposing that (3) remains invariant under rotations by π/s, one obtains $\alpha_x=\alpha_y$ and $\alpha_{xx}=\alpha_{yy}$ for any value of s. Additionally one finds $\alpha_{xx}=\alpha_{yy}=\alpha_{xy}/2$ whenever $s\geq 3$. As the linear part of the equation governing the envelope of the Bloch mode must coincide with the Fourier transform of (3) [12], we conclude that (2b) will be verified whenever $s\geq 3$. The applicability of (2b) to the case $s=2$ is however not granted.

We note that in the 1D case [$\mathbf{r}\to x$, $\nabla^2\to\partial^2/\partial x^2$, $s=1$ in (1)] the diffraction coefficients in (2) were calculated analytically [6,7] in the limit $f^2 \ll 1$ and $|1-\Omega_0| \ll 1$, which we exploit here as well. Indeed, a rigorous derivation of (2b) can be done by assuming that the modulation parameters in (1) verify

$$\Omega_0 = 1-\delta, \quad 4sf^2 = \delta^3 + \eta\delta^4, \quad (4)$$

$0<\delta\ll 1$ is a smallness parameter, and η is a quantity of order δ^0 which measures the deviation from "zero diffraction" [6,7]. One can then show (we skip the details, which follow the lines of [7]) that solutions to (1) exist that can be written as $\psi(\mathbf{r},t)=A(\mathbf{r},t)\psi_B(\mathbf{r},t)\exp(-i\bar{\Omega}t)+O(\delta^{5/4})$, where the envelope A is of order δ^2, the Bloch mode reads $\psi_B(\mathbf{r},t)=1-(\delta/s)^{1/2}V_s(\mathbf{r})\exp(-i\Omega_0 t)+O(\delta^{3/2})$, and $2\bar{\Omega}=-\delta^2+(1/2-\eta)\delta^3(1-\delta)$. We note that the Bloch mode above is the one with $\mathbf{K}=\mathbf{0}$ [7,12] as we are considering (almost) static solitons. The equation for A is found to depend on the symmetry parameter s, as expected. If $s\geq 3$, (2b) is obtained with $d_2=(2-\eta)\delta$ and $d_4=3/\delta^2$. In the square-symmetry case $s=2$ an equation similar to (2b) is obtained but with the term $d_4\nabla^4$ being replaced by $4\delta^{-2}(\partial^4/\partial x^4+\partial^4/\partial y^4)$, which does not possess rotational symmetry. These results are obtained going up to the order $\delta^{5/2}$ in a multiple scale analysis of (1) that uses $\delta^{1/2}$ as a smallness parameter [7]. At higher orders of the expansion the envelope equations for potentials with hexagonal ($s=3$) and octagonal ($s=4$) symmetries are no more equivalent (the former looses the rotational symmetry, while the latter still keeps it).

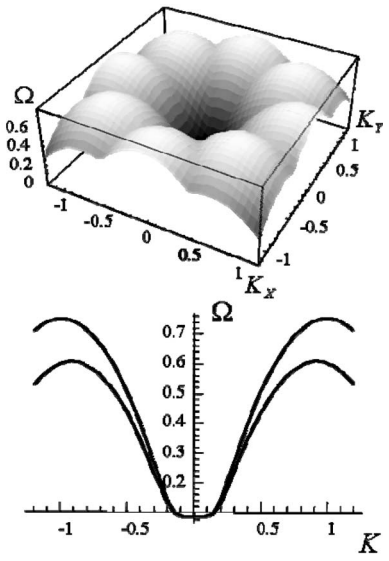

FIG. 1. Propagation constant (upper plot), and its cross section on $K_y=0$ axis, and the axis rotated by $\pi/8$ (lower plot), as obtained by a Bloch mode expansion of (1) for a quasiperiodic potential with $f=0.056$ and $\Omega_0=0.75$.

We concentrate on the following in the octagonal case $s=4$ (a quasiperiodic potential), which possesses improved rotational symmetry as compared to the hexagonal case $s=3$ as commented. By renormalizing the space as $(x',y')=3^{-1/4}\delta^{1/2}(x,y)$, one obtains (2b) as the envelope equation with $d_2=(2-\eta)\delta^2 3^{-1/2}$ and $d_4=1$. Note that for $\eta=2$ the purely subdiffractive case $d_2=0$ is obtained.

The dispersion relation $\Omega(\mathbf{K})$ for the linear Bloch modes of (1) was numerically determined by extending the analysis of [6,7] to two spatial dimensions. Figure 1 represents the lowest quasienergy surface in the octagonal case. We note the wide plateau around the origin, which signals subdiffraction [6,7].

We integrated numerically the microscopic model (1), using the octagonal quasiperiodic potential, with the parameters as in Fig. 1. We performed the calculations on a grid of 256×256 points by using the split step method. Solitons were seeded by using an initial condition for the field, $\psi(\mathbf{r},t=0)$, in the form of a Gaussian beam. Due to periodic modulation of the potential, as well as to the mismatch of the initial conditions with the true envelope of the solitons, radiation was observed. We used "softly absorbing" boundary conditions (simulated by a hyper-Gaussian function of losses) in the initial stage of the calculations in order to "absorb" the outgoing radiation, and then continued the calculations using periodic boundary conditions. An example of stable soliton of (1) is given in Fig. 2.

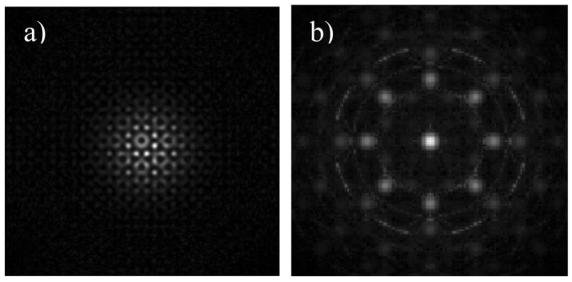

FIG. 2. Spatial profile of the soliton obtained by numerical solution of (1) with potential of octagonal symmetry in real space (a), and in Fourier space (b). The parameters are as in Fig. 1. The size of the integration region is $30\times 2\pi$.

After proving the stable solitons in the microscopic model (1) and after establishing the relation between microscopic (1) and macroscopic (2) models, we studied analytically and numerically solitons of (2). We keep below $d_4=1$ (without losing generality due to normalization of spatial coordinates), and consider three sets of coefficients: (i) $d_2=0$, which is the purely subdiffractive case; (ii) $d_2=1$, which corresponds to a nearly subdiffractive case, on the side of positive (normal) diffraction; and (iii) $d_2=-1$, which corresponds to a nearly subdiffractive case, on the side of negative diffraction (antidiffraction). As we are considering a nonlinearity with negative sign, the case $d_2<0$ ($d_2>0$) corresponds to weak focusing (defocusing). Numerical integrations of the NLSE (2b) were performed as described above, but now typically on a grid of 128×128 points, owed to its larger simplicity as compared with (1). Radially symmetric solitons were always found. Examples of stable solitons are given in Fig. 3. On the logarithmic scale the fringes around the solitons are clearly visible. These fringes are most strongly pronounced for the parameter range corresponding to the negative (and also for zero-) diffraction. On top of the fringes the

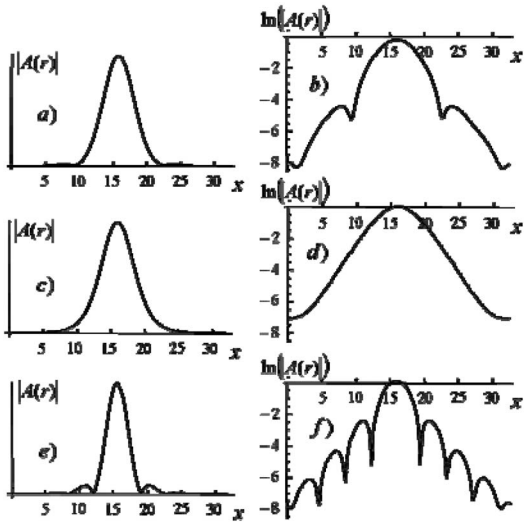

FIG. 3. Spatial profiles of the solitons obtained by numerical solution of (2b). The modulus of the field crossing the center of the solitons is depicted in linear (left) and linear-logarithmic (right) scales. The parameters are: (a),(b) $d_2=0$, (c),(d) $d_2=-1$, (e),(f) $d_2=1$.

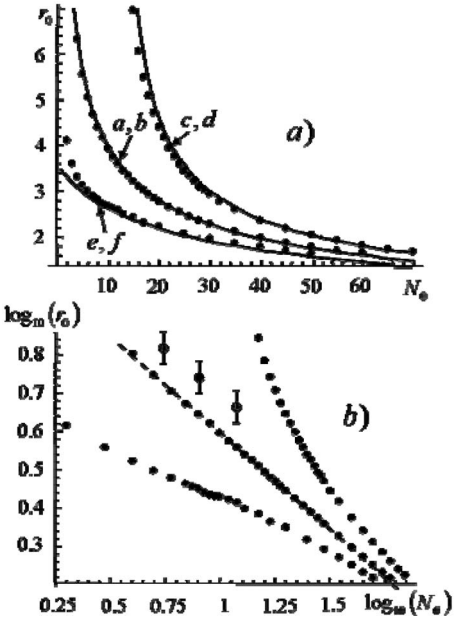

FIG. 4. The solitons width versus the number of particles in three different families of solitons corresponding to: $d_2=-1$ (upper curves), $d_2=0$ (middle curves), and $d_2=1$ (lower curves) in linear (a), and logarithmic (b) representation, as obtained by numerical integration of (2b). The dashed line in (b) corresponds to the power law $N_0r_0^2=$const as following from the scaling analysis. The solid lines in (a) are analytical evaluations (7). The circles with error bars in (b) denote solitons obtained by numerical solutions of (1) corresponding to $d_2=0$ (middle curves): The filled circle is for the solitons from Fig. 1, and the open circles are for the solitons from the same family but different form parameter.

slopes seem to follow an exponential decay law.

Next we plot the families of solitons in the (N_0,r_0) space, by calculating numerically the number of particles, and the full width of the soliton. We performed this procedure by "injecting" solitons of different width and amplitude, and again, filtering the outgoing radiation, getting finally a stationary solution. The families, corresponding to three sets of the parameters, are depicted in Fig. 3 in linear and logarithmic scales. The purely subdiffractive case results in a straight line in log-log scale, corresponding to the power law dependence obtained by the scaling analysis above. The weakly diffractive and antidiffractive cases do not correspond to a pure power law, and are estimated analytically below.

Next we reproduce analytically the curves in Fig. 4, and also perform the stability analysis using the Vakhitov-Kolokolov stability criterion. We look for a radially symmetric localized solution $A(\mathbf{r},t)=B(r)\exp(-i\mu t)$ of (2b) where μ is the propagation constant and $B(r)$ is the stationary envelope that corresponds to the minimum of the Hamiltonian

$$H=\int\left(d_2|\nabla B|^2-|\nabla^2 B|^2+\frac{|B|^4}{2}-\mu|B|^2\right)d^2r. \qquad (5)$$

We use the Gaussian ansatz $B(r)=A_0\exp[-(r/\Delta r)^2]$ with half width Δr and minimize (5) with respect to A_0 and Δr ($dH/dA_0=0$, $dH/d\Delta r=0$). This allows calculating the re-

lations between the soliton half width Δr and the number of particles in the soliton, $N_0=\frac{1}{2}\pi(\Delta r)^2A_0^2$ for a given propagation constant μ

$$N_0=-4\pi d_2+\frac{32\pi}{\Delta r^2},\quad \mu=-\frac{2d_2}{\Delta r^2}+\frac{24}{\Delta r^4}. \tag{6}$$

Equation (6) describes well the numerically calculated curves in Fig. 4 [note that the half width in the Gaussian ansatz Δr and the numerically calculated width r_0 related by $r_0=\Delta r(\pi/2)^{1/2}$]. Equation (6) predicts that these three curves are simply the horizontal translations of the one curve in the linear scale, since only parameter d_2 is different for them. Analysis of numerical data, Fig. 4(a), shows indeed that the curves with $d_2=0$ and $d_2=-1$ can be well matched by the horizontal translation. The matching of curves with $d_2=0$ and $d_2=1$ is worse at $N_0\to 0$, which corresponds to the breakup of the Gaussian ansatz (see the appearance of fringes in Fig. 3).

We also note good qualitative correspondence with the results of numerical integration of the full model (1), as indicated by circles with error bars in Fig. 4(b). The precise qualitative coincidence could be hardly expected since the smallness parameter is $\delta=0.25$, i.e., is not extremely small.

Equation (6) also indicates that for $d_2>0$ one can obtain solitons of finite width, but of extremely small number of the particles. The expression (6) for the propagation constant also leads to the values corresponding to the numerically ones found.

The Vakhitov-Kolokolov criterion [11] $\delta N_0/\delta|\mu|>0$ calculated from (6), $\delta N_0/\delta|\mu|\equiv(\delta N_0/\delta\Delta r)/(\delta|\mu|/\delta\Delta r)$, implies $d_4/(-d_2+24/\Delta r^2)>0$, and holds for arbitrary d_2. It does obviously for $d_2\leq 0$ and, as it becomes apparent considering (6), also for $d_2>0$.

The appearance of fringes follows from the linear analysis of the weak tails (slopes) of the solitons $A(r,t)=1/r\exp(-qr-i\mu t)$ leading to $q^2=(-d_2\pm\sqrt{d_2^2-4\mu})/2$. Thus for $d_2<-2\sqrt{\mu}$ results in the real values of decay exponents q (i.e., in nonoscillating fronts). For $d_2>0$ the values of q are nearly imaginary, which results in strongly oscillating fronts. This is well compatible with the numerics, where the fringes appear predominantly for $d_2>0$, but also (less pronounced) for $d_2=0$.

In conclusion, we propose a method for stabilizing NLSE solitons in 2D by means of a spatiotemporally modulated potential. Unlike other proposed methods based on spatial modulations of the potential (not spatiotemporal ones), which require the presence of a full 2D gap [3] and only work above a given soliton power (proportional to the particle number), the results presented here are not affected by those aspects.

We note that the Vakhitov-Kolokolov stability criterion also holds in the 3D case, as followed by the direct extension of our 2D analysis with the Gaussian ansatz and applying the scaling arguments. The numerical proof of solitons stability in the 3D case has however not been performed.

Our work financially supported by the Spanish Ministerio de Educación y Ciencia and the European FEDER through projects FIS2004-02587, FIS2005-07931-C03-01, and -03. We thank N. Akhmediev for discussions.

[1] E. A. Kuznetsov A. M. Rubenchik, and V. E. Zakharov, Phys. Rep. **142**, 103 (1986); K. Rypdal and J. J. Rasmussen, Phys. Scr. **40**, 192 (1989); L. Bergé, Phys. Rep. **303**, 259 (1998); Y. S. Kivshar and D. E. Pelinovsky, *ibid.* **331**, 117 (2000).

[2] N. Akhmediev and A. Ankiewicz, *Solitons, Nonlinear Pulses and Beams* (Chapman & Hall, London, 1997); Kh. I. Pushkarov and D. I. Pushkarov, Rep. Math. Phys. **17**, 37 (1980).

[3] N. K. Efremidis, J. Hudock, D. N. Christodoulides, J. W. Fleischer, O. Cohen, and M. Segev, Phys. Rev. Lett. **91**, 213906 (2003).

[4] V. Zharnitsky, E. Grenier, C. K. R. T. Jones, and S. K. Turitsyn, Physica D **152**, 794 (2001); F. Kh. Abdullaev, B. B. Baizakov, and M. Salerno, Phys. Rev. E **68**, 066605 (2003).

[5] O. Bang, W. Krolikowski, J. Wyller, and J. J. Rasmussen, Phys. Rev. E **66**, 046619 (2002).

[6] K. Staliunas and R. Herrero, Phys. Rev. E **73**, 016601 (2006).

[7] K. Staliunas, R. Herrero, and G. J. de Valcárcel, Phys. Rev. E **73**, 065603(R) (2006).

[8] For a BEC, parameters in (1) are $f=mV_0/(\hbar q_0)^2$ and $\Omega_0=2mv/(\hbar q_0)$, m being the atomic mass and v the common velocity of the moving lattices, which have wave number q_0 and potential depth V_0. Time and space are measured in units of $2m/\hbar q_0^2$ and q_0^{-1}, respectively.

[9] If the linear refractive index modulation of the PC is $n(\mathbf{r},z)=n_0[1+2m\cos(q_\parallel z)\Sigma_{j=1}^{s}\cos(\mathbf{Q}_j\cdot\mathbf{r})]$, with $|\mathbf{Q}_j|=q_\perp$ for all j, then parameters in (1) are: $f=m(k_0/q_\perp)^2$ and $\Omega_0=2k_0q_\parallel/q_\perp^2$, $k_0=n_0\omega_0/c$ being the light wave number and ω_0 its angular frequency. The propagation and transverse coordinates are measured in units of $2k_0/q_\perp^2$ and $q_\perp^{-1}$, respectively. The wave function $\psi=(-2n_2/n_0)^{1/2}(k_0/q_\perp)E$, $n_2<0$ being the nonlinear Kerr coefficient (in $m^2\,V^{-2}$) and E the light electric field complex envelope.

[10] V. I. Karpman, Phys. Rev. E **53**, R1336 (1996); V. I. Karpman and A. G. Shagalov, Physica D **144**, 194 (2000).

[11] M. G. Vakhitov and A. A. Kolokolov, Sov. Radiophys. **16**, 1020 (1973) [Radiophys. Quantum Electron.. **16**, 783 (1973)].

[12] C. M. de Sterke, D. G. Salinas, and J. E. Sipe, Phys. Rev. E **54**, 1969 (1996).